COMPUTATION OF ZERO-OFFSET VERTICAL SEISMIC PROFILES INCLUDING GEOMETRICAL SPREADING AND ABSORPTION*

B. URSIN and B. ARNTSEN**

ABSTRACT

URSIN, B. and ARNTSEN, B. 1985, Computation of Zero-Offset Vertical Seismic Profiles including Geometrical Spreading and Absorption, Geophysical Prospecting 33, 72–96.

Synthetic vertical seismic profiles (VSP) provide a useful tool in the interpretation of VSP data, allowing the interpreter to analyze the propagation of seismic waves in the different layers. A zero-offset VSP modeling program can also be used as part of an inversion program for estimating the parameters in a layered model of the subsurface.

Proposed methods for computing synthetic VSP are mostly based on plane waves in a horizontally layered elastic or anelastic medium. In order to compare these synthetic VSP with real data a common method is to scale the data with the spherical spreading factor of the primary reflections. This will in most cases lead to artificial enhancement of multiple reflections.

We apply the ray series method to the equations of motion for a linear viscoelastic medium after having done a Fourier transformation with respect to the time variable. This results in a complex eikonal equation which, in general, appears to be difficult to solve. For vertically traveling waves in a horizontally layered viscoelastic medium the solution is easily found to be the integral along the ray of the inverse of the complex propagation velocity. The spherical spreading due to a point source is also complex, and it is equal to the integral along the ray of the complex propagation velocity.

Synthetic data examples illustrate the differences between spherical, cylindrical, and plane waves in elastic and viscoelastic layered media.

INTRODUCTION

The computation of synthetic seismograms has proven to be an invaluable tool in correlating well log data with seismic data. The classical methods (Baranov and Kunetz 1960, Wuenschel 1960) are based on plane-wave propagation in a perfectly elastic horizontally layered medium. As shown by Trorey (1962), the effect of anelas-

tic absorption significantly changes the amplitudes and frequency content of the synthetic seismogram. Nielsen (1978) used a one-dimensional equation of motion for an anelastic medium to calculate synthetic seismograms for a source emitting plane waves. Ganley (1981) has done a similar calculation which includes the effect of absorption and dispersion of the seismic waves. Kennett (1979) used a two-dimensional Fourier-transform technique to compute synthetic seismograms for a line source. The phase-velocities used by Kennett are not frequency-dependent, though it can be shown that the principle of causality requires that wave propagation in absorptive media is dispersive (Aki and Richards 1980).

The extension of these classical methods to the computation of synthetic vertical seismic profiles (VSP) is straightforward (Wyatt 1981). Synthetic vertical seismic profiles provide a useful tool in interpretation of VSP data since they allow the interpreter to analyze the propagation of seismic waves in different layers and to study the effects of primary and multiple reflections (Balch, Lee, Miller and Ryder 1982). Proposed techniques for computing synthetic VSP are plane waves in an elastic medium with constant two-way traveltime in each layer (Wyatt 1981) and plane waves in an anelastic layered medium with homogeneous layers (Kan, Corrigan and Huddleston 1981). The last mentioned method is based on a recursive technique for solving the one-dimensional wave equation in the frequency domain.

In most practical cases the source is a point source, and the effect of geometrical spreading has to be taken into account. In order to compare the synthetic seismograms computed for a plane-wave source with real data, it is common to scale the data with the geometrical spreading factor computed for primary reflections. This procedure leads in many cases to artificial enhancement of the multiple reflections. In order to include both anelasticity and geometrical spreading in the calculation of synthetic seismograms, an equation of motion and an appropriate solution are needed. We shall use the equations of motion for a viscoelastic medium (Ben-Menahem and Singh 1981) and, after a Fourier transformation with respect to the time variable, we shall apply the ray-series method (Červený and Hron 1980). A different approach based on the ray-series method has been used by Buchen (1974). In appendix A we show that our approach results in a complex eikonal equation which apparently is difficult to solve for a general inhomogeneous medium. For vertically traveling waves in a horizontally layered viscoelastic medium a solution can be found (see appendix B). The solution of the complex eikonal equation is obtained by integrating the inverse of the complex velocity along the ray. By computing the amplitudes corresponding to a point source, it is seen that the geometrical spreading factor now is complex, and it is equal to the integral of the complex velocity along the ray. This extends a well-known result derived by Newman (1973) for a horizontally layered elastic medium. The amplitudes of waves generated by a line source can be computed by using the square root of the geometrical spreading factor for spherical waves. For plane waves there is, of course, no geometrical spreading.

In appendix C we apply the usual boundary conditions at an interface between two inhomogeneous viscoelastic media to derive the transmission and reflection coefficients for spherical, cylindrical, and plane waves. We also derive a frequency-

independent approximation of the reflection and transmission coefficients. In appendix D we discuss our choice of complex propagation velocity (Aki and Richards 1980).

The results are summarized in the main text where we also give an approximative method for computing synthetic VSP which is computationally efficient. The ray generation algorithm is similar to the ones used by Hron (1972) and Vetter (1981).

The difference between spherical, cylindrical, and plane waves, and between elastic and viscoelastic media is illustrated with synthetic data examples.

ZERO-OFFSET RAY SERIES FOR A LAYERED VISCOELASTIC MEDIUM

We consider a horizontally stratified viscoelastic medium consisting of N layers bounded by two half-spaces. The layers are numbered from 0 to $N + 1$, where layer number 0 and $N + 1$ are the half-spaces at the top and bottom of the medium. We define a coordinate system with the z-axis vertically downwards. The coordinate of interface number k at the bottom of layer number k is z_k, and we choose $z_0 = 0$.

An approximate solution of the equations of motion can be found by expanding the displacement or displacement velocity in a ray series as shown in appendix A. This results in a complex eikonal equation which is, in general, difficult to solve. For vertically traveling waves a simple solution can be found. In appendix B it is shown that the displacement can be expressed as a sum of terms corresponding to all primary and multiple reflected waves. We consider a source at $z = z_s$, where the displacement velocity is given. Unless $z_s = 0$, both upgoing and downgoing waves are generated by the source. We let the displacement velocity be positive along the direction of the ray so that the upgoing and downgoing wave have the same polarity for explosive sources. We let s denote arclength along the ray with $s = 0$ at the source. The receiver is at z_r located in an arbitrary layer (but at the same lateral position as the source). At the receiver we compute the displacement velocity in the z-direction which is positive for a downgoing wave and negative for an upgoing wave. Combining the results from appendix B and C we obtain the displacement velocity as a sum of terms of the form

$$V(s, \omega) = \prod_{j=1}^{N_j} \sqrt{\left(\frac{\rho(z_{j+})A(z_{j+}, \omega)}{\rho(z_{j+1-})A(z_{j+1-}, \omega)}\right)} F(s, \omega)V_0(\omega)$$
$$\prod_n R_n(\omega) \prod_k T_k(\omega) \exp[i\omega\tau(s, \omega)], \qquad (1)$$

where z_{j+} is the coordinate at the top of layer number $j + 1$ and z_{j+1-} is the coordinate at the bottom of layer number $j + 1$, $\rho(z)$ is the density, and

$$A(z, \omega) = C_r(z) \frac{1 + \dfrac{1}{\pi Q} \log \dfrac{\omega}{\omega_r}}{1 + \dfrac{i}{2Q}} \qquad (2)$$

is the complex propagation velocity (see appendix D). The product over j in (1) is to be taken over all layers passed by the ray starting at the source, $z_{1+} = z_s$, and ending at the receiver, $z_{N+1-} = z_r$. The factors introduced when passing a layer both upwards and downwards cancel, and the product contains only terms due to the layers between the source and receiver. This product is therefore independent of the type of wave, and it can be taken out of the summation and computed only once. Furthermore, the factors due to homogeneous layers are equal to one. $V_0(\omega)$ is the source displacement velocity at $s = 1$ m, but with the delay due to the 1 m separation removed. $F(s, \omega)$ is a factor which takes the geometrical spreading into account. We have

$$F(s, \omega) = \left\{ \frac{A(0, \omega)}{n(s, \omega)} \right\}^k \tag{3}$$

with

$$n(s, \omega) = \int_0^s A(\sigma, \omega) \, d\sigma \tag{4}$$

and

$$k = \begin{cases} 1 \text{ for a point source,} \\ \tfrac{1}{2} \text{ for a line source,} \\ 0 \text{ for a plane source.} \end{cases} \tag{5}$$

The phase function $\tau(s, \omega)$ is the solution of the complex eikonal equation. It is given by

$$\tau(s, \omega) = \int_0^s \frac{d\sigma}{A(\sigma, \omega)}. \tag{6}$$

The products of $R_n(\omega)$ and $T_k(\omega)$ contain all reflection and transmission coefficients which take into account the boundary conditions at the interfaces between the different layers. In appendix C it is shown that the transmission coefficient is

$$T(\omega) = 1 - R(\omega) \tag{7}$$

and, for a downward traveling wave incident at z_k, the reflection coefficient is

$$R(\omega) = \frac{G(z_{k+}, \omega) - G(z_{k-}, \omega)}{G(z_{k+}, \omega) + G(z_{k-}, \omega)}, \tag{8}$$

where

$$G(z, \omega) = \rho(z)A(z, \omega) \left[1 - k \frac{A(z, \omega)^2}{i\omega n(s, \omega)} \right] \tag{9}$$

with k defined in (5) and $n(s, \omega)$ given in (4). The second term in (9) is a near-field term (Berkhout 1982, p. 93) which will not be included in the approximate computations discussed below.

In the computations we shall assume that the reference velocity at ω_r, C_r in (2) is a linear function of depth in each layer:

$$C_{rk}(z) = C_k + g_k(z - z_{k-1}) \tag{10}$$

for $z_{k-1+} \leq z \leq z_{k-}$. C_k is the velocity at the top of layer number k, and g_k is the velocity gradient in the layer. With this velocity function we can now integrate the functions $n(s)$ and $\tau(s)$ over layer number k to obtain the contribution to the sums in (4) and (6) due to the passage of the wave through this layer. We obtain

$$\Delta n_k = \int_{z_{k-1}}^{z_k} A(\sigma) \, d\sigma$$

$$= [C_k D_k + \tfrac{1}{2} g_k D_k^2] \left[\frac{1 + \dfrac{1}{\pi Q_k} \log \dfrac{\omega}{\omega_r}}{1 + \dfrac{i}{2Q_k}} \right]^{-1}, \tag{11}$$

where $D_k = z_k - z_{k-1}$ is the thickness of layer number k, and Q_k is constant in the layer. We also obtain

$$\Delta \tau_k = \int_{z_{k-1}}^{z_k} \frac{d\sigma}{A(\sigma)} = \frac{1 + \dfrac{1}{\pi Q_k} \log \dfrac{\omega}{\omega_r}}{1 + \dfrac{i}{2Q_k}} \cdot h_k, \tag{12}$$

where

$$h_k = \begin{cases} \dfrac{D_k}{C_k} & \text{if } g^k = 0, \\[3mm] \dfrac{1}{g_k} \log \left(1 + \dfrac{D_k g_k}{C_k} \right) & \text{if } g_k \neq 0. \end{cases} \tag{13}$$

In some cases the source generates a pressure pulse $P_0(\omega)$, or the receiver records pressure. To convert from pressure to displacement velocity or vice versa, we shall use the relation (see appendix C)

$$S_{33}(\omega) = \pm \rho A i \omega \left(1 - k \frac{A^2}{i\omega n} \right) U^3(\omega), \tag{14}$$

where S_{33} is the Fourier transform of the stress σ_{33} and U_3 is the Fourier transform of the vertical displacement. The factor k depends on the type of source and is given in (5). In (14) the plus sign is used for downward traveling waves and the minus sign for upward traveling waves. With the same sign convention we have that in (1) $V = \pm V_3$, and we also have $V_3 = -i\omega U_3$ and $P = -S_{33}$. Thus, (14) gives

$$P = \rho A \left(1 - k \frac{A^2}{i\omega n} \right) V. \tag{15}$$

In the computations we always use the far-field approximation $P = \rho A V$.

Approximate Computation of the Ray Series

In the preceding section we have given an exact representation of the ray series in a layered viscoelastic medium. The complex functions $n(\sigma, \omega)$ and $\tau(\sigma, \omega)$ must be computed for all frequencies in the frequency band of the input signal, and the reflection and transmission coefficients must also be computed for each frequency. Since this must be done for each ray, and the number of rays is large, the exact computations are very expensive in terms of computer time. In order to speed up the computations we have made certain approximations.

The reflection coefficients are approximated by (see appendix C)

$$R = \frac{G_0(z_{k+}) - G_0(z_{k-})}{G_0(z_{k+}) + G_0(z_{k-})}, \tag{16}$$

where now

$$G_0(z) = \frac{\rho C_r(z)}{1 + \dfrac{i}{2Q}} \tag{17}$$

is frequency-independent. This approximation is also used when the transmission coefficient in (7) is computed.

In the computation of $n(s, \omega)$ and $\tau(s, \omega)$ we use the approximations

$$n(s, \omega) = \sum_k [C_k D_k + \tfrac{1}{2} g_k D_k^2] \frac{1 + \dfrac{1}{\pi Q_k} \log \dfrac{\omega}{\omega_r}}{1 + \dfrac{i}{2Q_k}}$$

$$\approx \left[1 + \frac{1}{\pi Q_{av}} \log \frac{\omega}{\omega_r}\right] \sum_k \frac{C_k D_k + \tfrac{1}{2} g_k D_k^2}{1 + \dfrac{i}{2Q_k}} \tag{18}$$

and

$$\tau(s, \omega) = \sum_k h_k \frac{1 + \dfrac{i}{2Q_k}}{1 + \dfrac{1}{\pi Q_k} \log \dfrac{\omega}{\omega_r}}$$

$$\approx \left[1 + \frac{1}{\pi Q_{av}} \log \frac{\omega}{\omega_r}\right]^{-1} \sum_k h_k \left(1 + \frac{i}{2Q_k}\right). \tag{19}$$

h_k is defined in (13), and the average value of Q is given by

$$\frac{1}{Q_{av}} = \frac{\sum_k D_k/Q_k}{\sum_k D_k}. \tag{20}$$

In (18)–(20) all sums over k are extended over all layers passed by the ray (that is, a given layer may be included several times for a multiple reflection).

When the variation in Q in the model is not too large, these simplifications give acceptable results. In the next section the errors have been computed for a simple model. We refer to this approximation as the "average attenuation approximation".

NUMERICAL RESULTS

In this section we present synthetic seismograms computed for simple models demonstrating the effects of geometrical spreading and absorption. The total wave-field (displacement velocity or pressure) is obtained as an infinite sum of rays, each contributing an amount given by (1). For practical calculations the number of rays must be limited to a finite number. One way of doing this is to group the rays according to the number of reflections they have gone through (Vetter 1981), and then carry out the calculations until all rays with a certain reflection order (i.e., all rays with a certain number of reflections) have been included. In the following numerical examples all rays with one to five reflections have been included. The examples showing single traces have been computed with an airgun source and recorded with a hydrophone, both located 7.5 m below the surface.
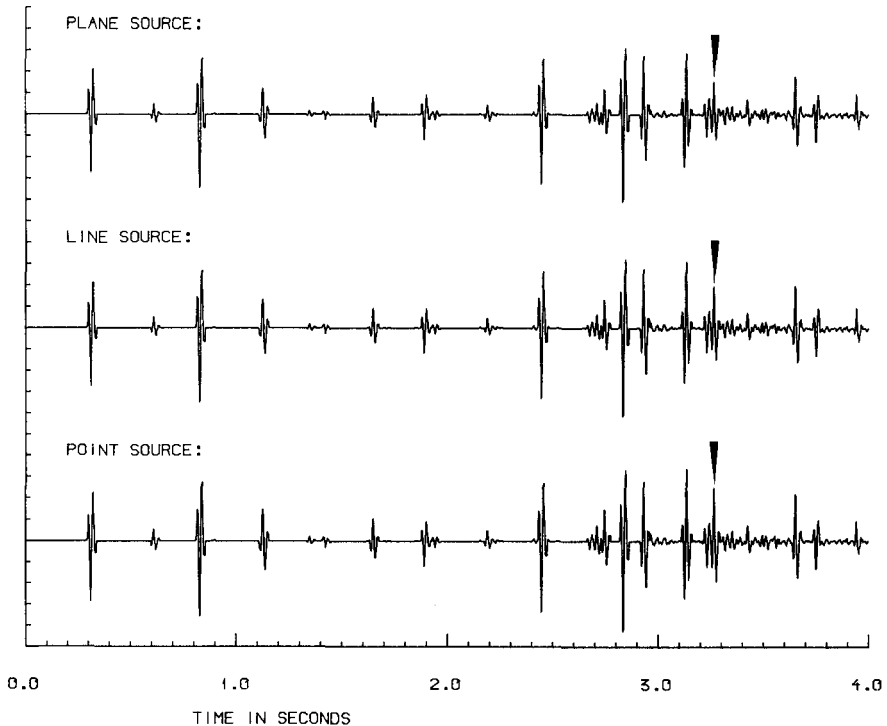

Fig. 1. Seismograms computed for the model defined in table 1, assuming a perfectly elastic medium.

Table 1. *Parameters for the model used for the computation of seismograms with different sources.*

Layer no.	Velocity (m/s)	Dimensions (m)	Q-value	Density (g/cm^3)
0	0.0	—	10 000.0	0.0
1	1500.0	225.0	10 000.0	1.09
2	1615.0	419.0	50.0	1.46
3	2050.0	300.0	100.0	1.86
4	1950.0	750.0	100.0	1.77
5	2160.0	600.0	100.0	1.90
6	3050.0	350.0	200.0	2.20
7	3165.0	250.0	200.0	2.25
8	5350.0	260.0	200.0	2.57
9	3600.0	350.0	200.0	2.35
10	4770.0	—	200.0	2.47

Figure 1 shows different seismograms computed for the model defined in table 1, but the layers are assumed to be perfectly elastic. This corresponds to infinite Q in each layer. In order to compare the response for different sources, the seismograms have been scaled with the inverse of the geometrical spreading factor of the primary reflections by multiplying with the function

$$
B(t) = \begin{cases}
\dfrac{1}{F_1} & 0 \le t \le t_1 \\[2ex]
\dfrac{1}{F_k} + \dfrac{t - t_k}{t_{k+1} - t_k}\left(\dfrac{1}{F_{k+1}} - \dfrac{1}{F_k}\right), & \begin{array}{l} t_k \le t \le t_{k+1} \\ k = 1, 2, \ldots, N-1 \end{array} \\[2ex]
\dfrac{1}{F_N} & t \ge t_N
\end{cases}
\tag{21}
$$

where F_k is the geometrical spreading factor defined in equation (3) for the primary reflection number k arriving at time t_k. We note that $B(t) = 1$ for a plane-wave source. In fig. 1 the top response is for a plane-wave source, the middle response is for a line source, and the bottom response is for a point source. The scaling of the responses has partly compensated for the geometrical spreading for point and line sources, so that these scaled responses are approximately equal to the plane-wave response, but the multiple reflections have not been properly scaled as indicated by the arrows. This is shown more clearly in fig. 2, where the difference between the plane- and the point-source responses are plotted at the top, the difference between the plane- and the line-source responses is plotted in the middle, and the difference between the line- and the point-source responses is plotted at the bottom. We note that due to the linear interpolation in (21) and the finite pulse length, the primary reflections have also been improperly scaled.

Figure 3 shows various responses computed for the model defined in table 2. All responses have been computed for a point source and then scaled according to (21).

PLANE – POINT:

PLANE – LINE:

LINE – POINT:

0.0　　　　　　　1.0　　　　　　　2.0　　　　　　　3.0　　　　　　　4.0
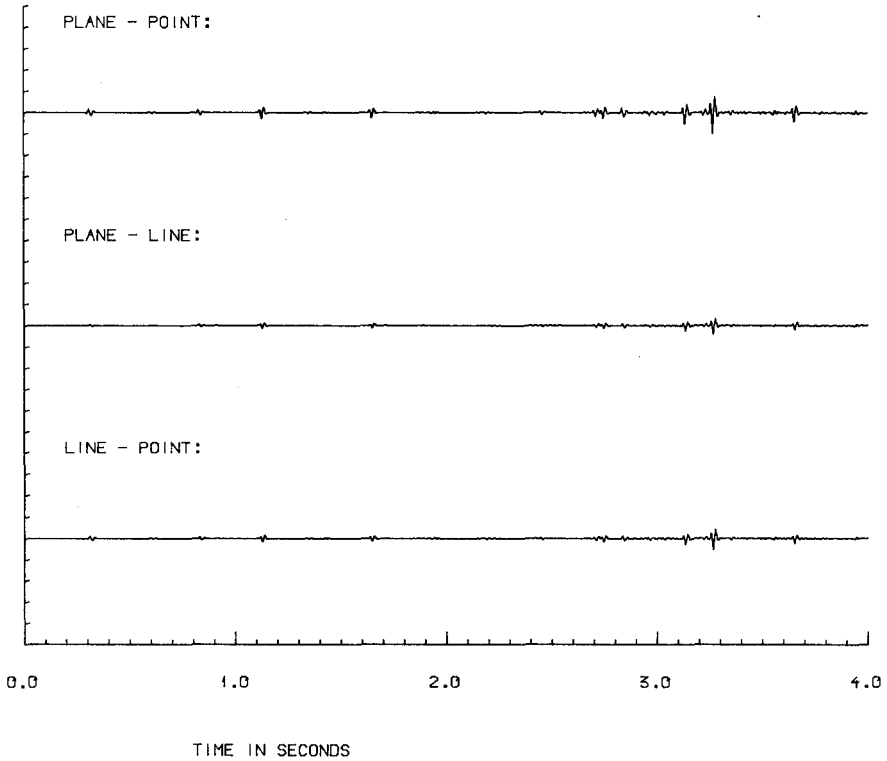
TIME IN SECONDS

Fig. 2. Differences between the seismograms shown in fig. 1.

The response plotted at the top is the response of a perfectly elastic medium, and the next response is the complete anelastic response computed according to (1). We see that the effect of anelastic attenuation is to reduce the amplitudes of the reflected pulses significantly. The next response has also been computed for an anelastic medium, but now the plane-wave reflection coefficients have been used ($k = 0$ in (9)). The difference between the exact anelastic response and this response has been plotted at the bottom of fig. 4. We see that using the plane-wave reflection and

Table 2. *Parameters for the simplified model used for the comparison of calculation methods.*

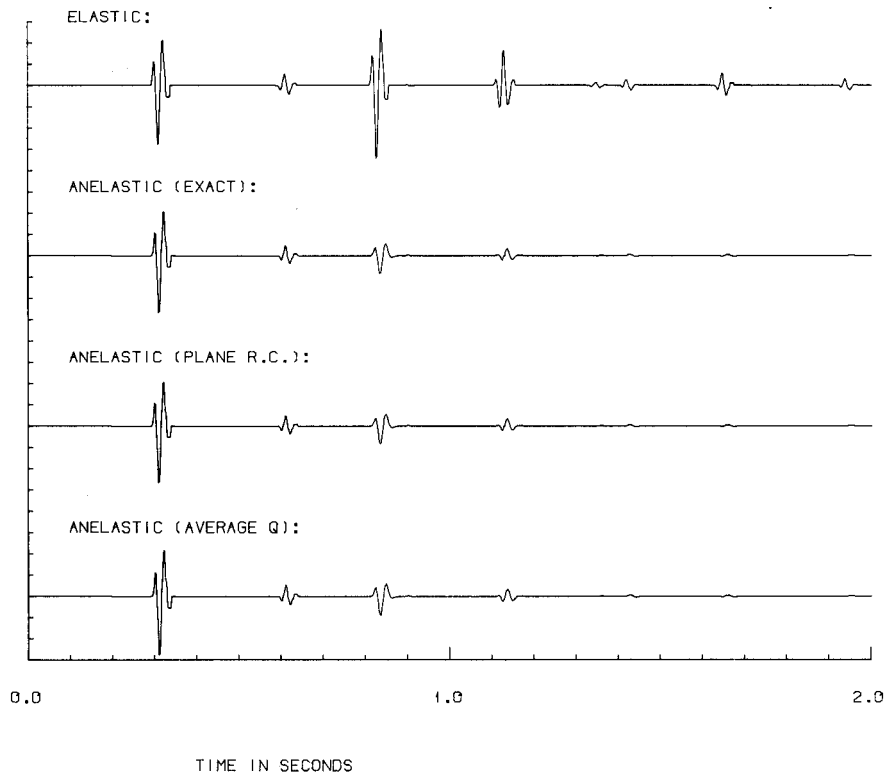| Layer no.	Velocity (m/s)	Dimensions (m)	Q-values	Density (g/cm^3)
0	0.0	—	10 000.0	0.0
1	1500.0	225.0	10 000.0	1.09
2	1615.0	419.0	50.0	1.46
3	2050.0	300.0	100.0	1.86
4	2250.0	—	100.0	1.90

Fig. 3. Seismograms computed for the model defined in table 2.

transmission coefficients introduces very small errors in the seismogram computed for this model.

At the bottom of fig. 3 we have plotted the approximate response computed with the frequency-independent reflection and transmission coefficients given in (16) and (17), and the average attenuation given in (18) to (20). The difference between this approximate response and the complete response is plotted at the top of fig. 4. We see that within the plotting scale, this is a useful approximation, and we expect this approximation to give good results when we compare synthetic responses with real data.

The average attenuation approximation discussed above results in a large reduction in CPU-time needed to run the program on a computer. On a Norsk Data ND560 the complete anelastic response required 435 s, the response with plane-wave reflection and transmission coefficients required 254 s, and the average attenuation response required 28 s.

In fig. 5 we have plotted the responses of the model defined in table 1, and now we have assumed that all layers are viscoelastic. The responses were computed for plane, line, and point sources and then corrected for geometrical spreading by

EXACT – AVERAGE Q:

(EXACT – AVERAGE Q)×10:

EXACT – PLANE R.C.:

(EXACT – PLANE R.C.)×100:

0.0   1.0   2.0
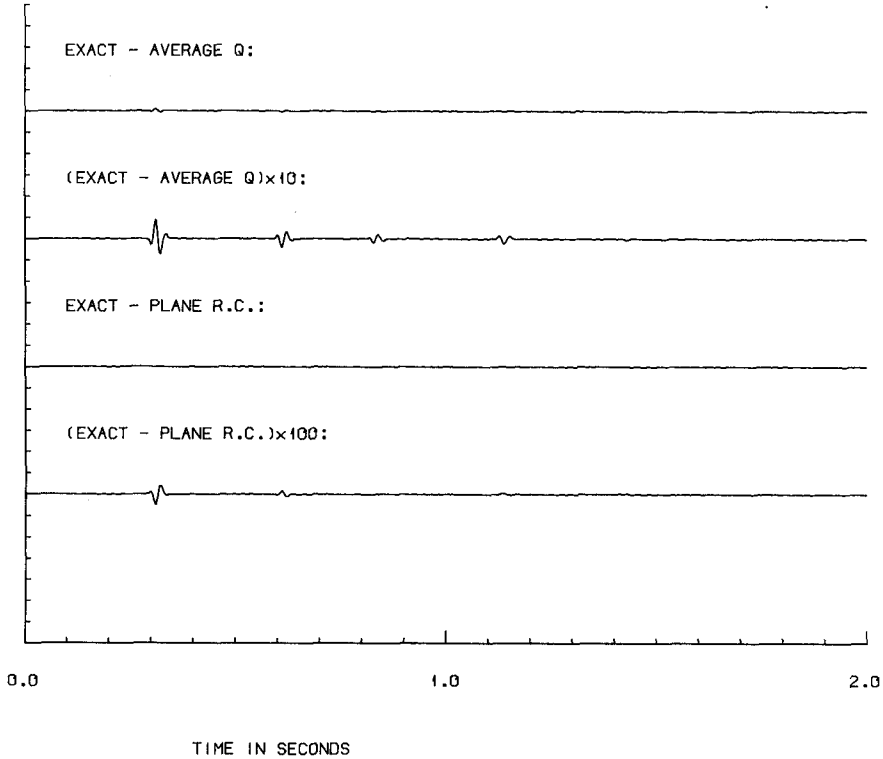
TIME IN SECONDS

Fig. 4. Differences between the seismograms shown in fig. 3.

multiplying with the scaling function defined in (21). Due to the effect of the anelastic attenuation, the amplitudes of the responses at times greater than about 2 s were below the plotting scale (see fig. 3). The responses plotted in fig. 5 have therefore also been exponentially scaled by multiplying with $\exp(t/t_0)$, where t is time in seconds. Keeping this scaling in mind the responses in fig. 5 can be compared with the corresponding responses in fig. 1 for an elastic medium. The anelastic attenuation significantly reduces the amplitudes of the late reflections, and since the high frequencies are most attenuated, the reflected pulses have a broader pulse-shape.

Figure 6 shows the differences between the responses plotted in fig. 5. At the top the difference between the responses for a plane and a point source has been plotted. The response in the middle shows the difference between a plane and a line source, and at the bottom the difference between a line and a point source has been plotted. We see that the amplitudes of the multiple reflections differ for the different source types.

In figs 7 and 8 we have plotted zero-offset VSP for the model given in table 3. The VSP response shown in fig. 7 is for a perfectly elastic medium, while the response shown in fig. 8 shows the effect of anelastic attenuation. For plotting purposes a time-variant, data-adaptive scaling has been used. Using a sliding time-
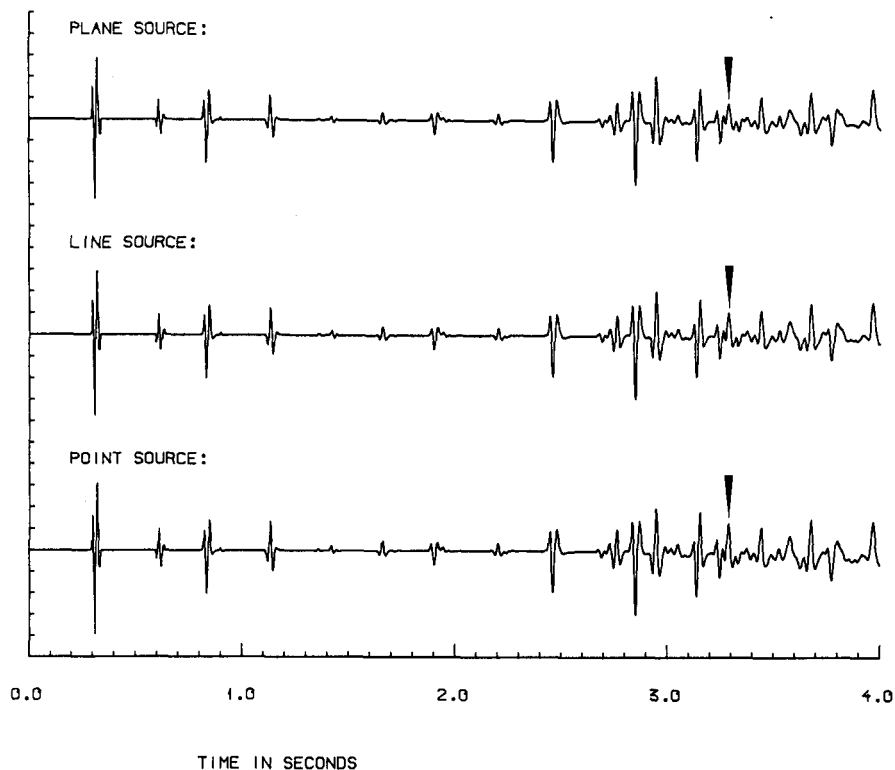
Fig. 5. Seismograms computed for the model defined in table 1, assuming all layers to be viscoelastic.

window, the traces have been scaled so that the sum of the absolute values of the response within the window is constant. This means that the amplitude information in figs 7 and 8 is significantly reduced. We see that the effect of the anelastic attenuation is to reduce the high-frequency content of the response.

CONCLUSION

We have shown that realistic seismic responses should include the effect of geometrical spreading and anelastic attenuation. Further investigations are needed to find the exact form of the attenuation mechanism, and to estimate the unknown parameters in the equations.

ACKNOWLEDGMENT

PLANE – POINT:

PLANE – LINE:

LINE – POINT:

0.0   1.0   2.0   3.0   4.0
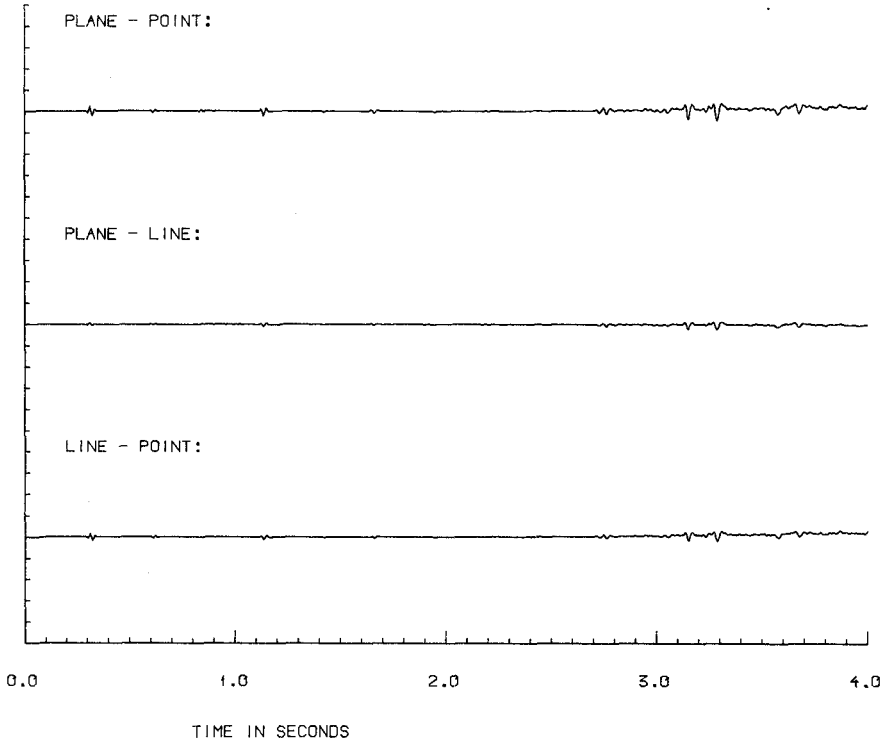
TIME IN SECONDS

Fig. 6. Differences between the seismograms shown in fig. 5.

Table 3. *Parameters for the model used for the computation of zero-offset VSP.*

Layer no.	Velocity (m/s)	Dimensions (m)	Q-value	Density (g/cm^3)
0	0.0	—	10 000.0	0.0
1	1500.0	225.0	50.0	1.03
2	1970.0	705.0	70.0	2.0
3	2200.0	245.0	100.0	2.0
4	2000.0	135.0	100.0	1.9
5	2200.0	390.0	100.0	1.9
6	2400.0	125.0	200.0	2.1
7	2600.0	200.0	200.0	2.2
8	2800.0	375.0	200.0	2.3
9	3000.0	150.0	250.0	2.4
10	3200.0	250.0	250.0	2.5
11	3000.0	60.0	200.0	2.4
12	3200.0	40.0	200.0	2.4
13	3100.0	130.0	200.0	2.5
14	3200.0	—	250.0	2.6

TRAVELTIME (SEC)

DEPTH (KM)
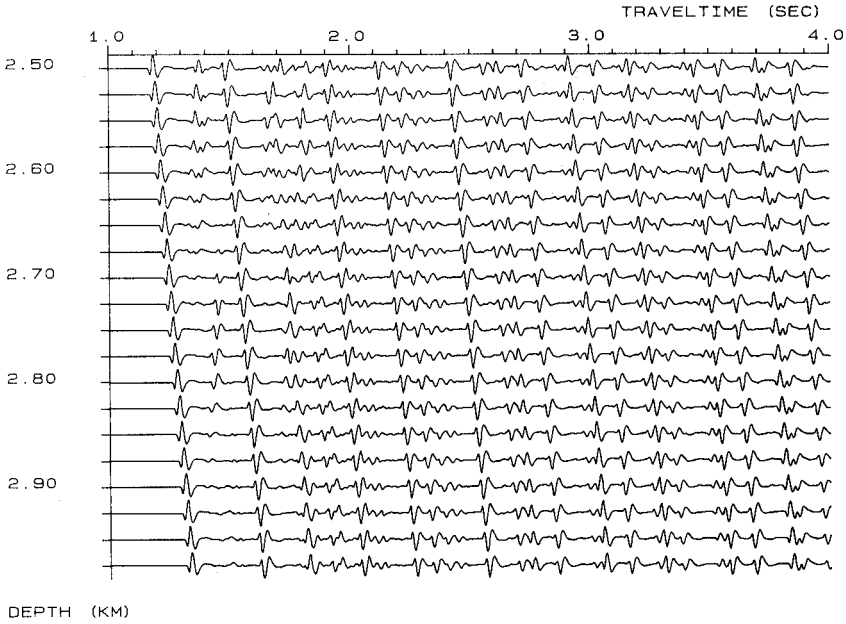
Fig. 7. Zero-offset VSP for the model defined in table 3, assuming a perfectly elastic medium.
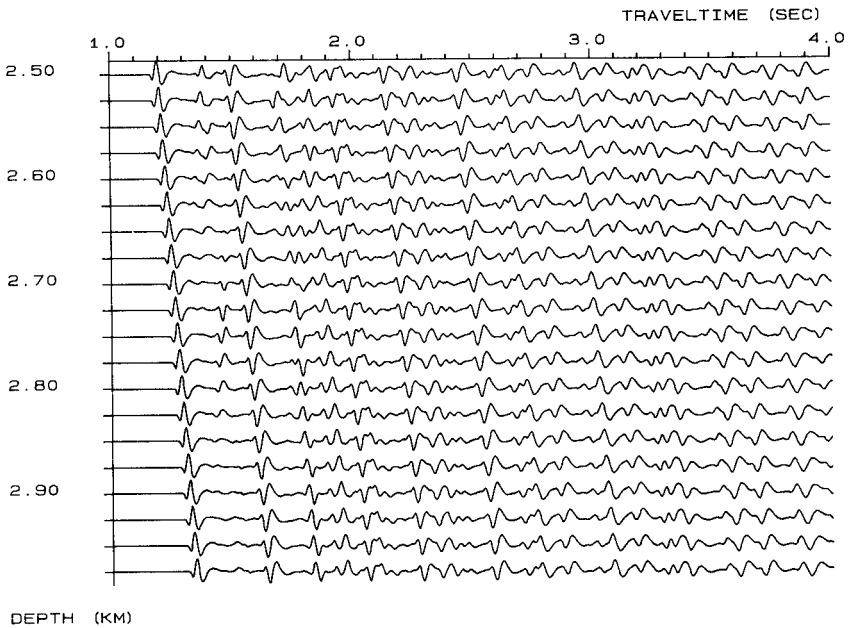
TRAVELTIME (SEC)

DEPTH (KM)

Fig. 8. Zero-offset VSP for the model defined in table 3, assuming all layers to be viscoelastic.

Appendix A

The Ray-Series Method Applied to Linear Viscoelastic Media

We let $\mathbf{x} = (x_1, x_2, x_3)$ be a fixed coordinate system with the x_3-axis positive downwards. We consider a linear viscoelastic medium with stress–strain relation (using the Einstein summation rule):

$$\sigma_{ij}(\mathbf{x}, t) = 2\mu * \varepsilon_{ij} + \delta_{ij}\lambda * \varepsilon_{mm}, \tag{A1}$$

where $\sigma_{ij}(x, t)$ is the stress tensor,

$$\delta_{ij} = \begin{cases} 1 & i = j \\ 0 & i \neq j \end{cases} \tag{A2}$$

is the Kronecker symbol, and ε_{ij} is the strain tensor defined by

$$\varepsilon_{ij}(\mathbf{x}, t) = \tfrac{1}{2}[u_{i,j}(\mathbf{x}, t) + u_{j,i}(\mathbf{x}, t)], \tag{A3}$$

where

$$\mathbf{u}(\mathbf{x}, t) = [u_1(\mathbf{x}, t), u_2(\mathbf{x}, t), u_3(\mathbf{x}, t)]$$

is the particle displacement vector, and the partial derivatives are denoted by

$$u_{i,j}(\mathbf{x}, t) = \frac{\partial u_i(\mathbf{x}, t)}{\partial x_j}. \tag{A4}$$

μ and λ are space-variant convolution operators of the type

$$(\mu * \varepsilon_{ij})(\mathbf{x}, t) = \int_0^t \mu(\mathbf{x}, \tau)\varepsilon_{ij}(\mathbf{x}, t - \tau)\,\mathrm{d}t \tag{A5}$$

corresponding to the Lamé parameters. The equations of motion are

$$\rho u_{i,tt} = \sigma_{ij,j}, \tag{A6}$$

where $\rho(x)$ is the density. From (A1) to (A6) we obtain

$$\rho u_{i,tt} = (\lambda + \mu) * u_{j,ij} + \mu * u_{i,jj} + \lambda_{,i} * u_{j,j} + \mu_{,j} * (u_{i,j} + u_{j,i}), \tag{A7}$$

which are the general equations of motion for a linear viscoelastic medium of Boltzman type (Ben-Menahem and Singh 1981).

We derive the ray series solution of (A7) using the approach of Červený and Hron (1980). The displacement vector is written in the form of a ray series:

$$u_i(\mathbf{x}, t) = \sum_{k=0}^{\infty} U_i^{(k)}(\mathbf{x})f_k(t - \tau(\mathbf{x})), \tag{A8}$$

where $f_k(t)$ are complex functions satisfying $f'_k(t) = \mathrm{d}f_k/\mathrm{d}t = f_{k-1}(t)$, and such that the real and imaginary parts of $f_k(t)$ constitute Hilbert transorm pairs of functions.

We shall use the Fourier transform

$$U_i(\mathbf{x}, \omega) = \int_{-\infty}^{\infty} u_i(\mathbf{x}, t) \exp(i\omega t)\, dt \tag{A9}$$

to transform the ray series (A8) into

$$U_i(\mathbf{x}, \omega) = \exp[i\omega\tau(\mathbf{x})] \sum_{k=0}^{\infty} U_i^{(k)}(\mathbf{x}) F_k(\omega). \tag{A10}$$

When we apply the Fourier transform to (A7) we obtain

$$-\rho\omega^2 U_i = (\Lambda + M)U_{j,ij} + MU_{i,jj} + \Lambda_{,i}U_{j,j} + M_{,j}(U_{i,j} + U_{j,i}), \tag{A11}$$

where the Fourier transforms of λ and μ are Λ and M, respectively. We use equation (A10) in (A11) and note that $F_{k-1}(\omega) = -i\omega F_k(\omega)$. By comparing equal powers of ω we obtain the operator equation (Červený and Hron 1980, equation (14))

$$NU^{(k)} - KU^{(k-1)} + LU^{(k-2)} = 0, \qquad k = 0, 1, \ldots, \tag{A12}$$

with $U^{(-1)} = U^{(-2)} = 0$. The operators are (in component form):

$$\begin{aligned}
N_i U^{(k)} &= -\rho U_i^{(k)} + (\Lambda + M)U_j^{(k)}\tau_{,i}\tau_{,j} + MU_i^{(k)}\tau_{,j}\tau_{,j}, \\
K_i U^{(k)} &= (\Lambda + M)[U_{j,i}^{(k)}\tau_{,j} + U_{j,j}^{(k)}\tau_{,ij} + U_j^{(k)}\tau_{,ij}] \\
&\quad + M[2U_{i,j}^{(k)}\tau_{,j} + U_i^{(k)}\tau_{,jj}] \\
&\quad + \Lambda_{,i}U_j^{(k)}\tau_{,j} + M_{,j}[U_i^{(k)}\tau_{,j} + U_j^{(k)}\tau_{,i}], \\
L_i U^{(k)} &= (\Lambda + M)U_{j,ij}^{(k)} + MU_{i,jj}^{(k)} \\
&\quad + \Lambda_{,i}U_{j,j}^{(k)} + M_{,j}[U_{i,j}^{(k)} + U_{j,i}^{(k)}].
\end{aligned} \tag{A13}$$

The first equation is $NU^{(0)} = 0$ which gives the eikonal equations

$$\tau_{,j}\tau_{,j} = \frac{1}{A^2} \tag{A14.a}$$

and

$$\tau_{,j}\tau_{,j} = \frac{1}{B^2}, \tag{A14.b}$$

where

$$A^2 = \frac{\Lambda + 2M}{\rho} \tag{A15.a}$$

and

$$B^2 = \frac{M}{\rho} \tag{A15.b}$$

are the squared (complex) velocities for P- and S-waves, respectively.

The solution of the complex eikonal equation is not straightforward, except in the case of vertically traveling waves in a horizontally layered medium. This case is treated in appendix B. We note that the derivation in Červený and Hron (1980) can formally be followed until their (23), but that the equivalent of (24) is not generally true.

Appendix B

Vertically Traveling Waves in a Horizontally Layered Viscoelastic Medium

We consider vertically traveling P-waves in a horizontally layered viscoelastic medium. The ray direction is $\mathbf{m} = \pm \mathbf{e}_3$, where $\mathbf{e}_3$ is a unit vector in the x_3-direction (vertically downwards). In this case the complex eikonal equation (A14.a) has the solution

$$\nabla \tau = \frac{1}{A} \cdot \mathbf{m}, \tag{B1}$$

which gives

$$\tau(s, \omega) = \tau(s_0, \omega) + \int_{s_0}^{s} \frac{d\sigma}{A(\sigma, \omega)}, \tag{B2}$$

where s is the length of the ray path. We decompose the amplitude components into two vector components:

$$\mathbf{U}^{(k)} = \mathbf{U}_{\|}^{(k)} + \mathbf{U}_{\perp}^{(k)}, \tag{B3}$$

where

$$\mathbf{U}_{\|}^{(k)} = U_p^{(k)} \mathbf{m} \tag{B4.a}$$

and

$$\mathbf{U}_{\perp}^{(k)} = U_{s1}^{(k)} \mathbf{e}_1 + U_{s2}^{(k)} \mathbf{e}_2. \tag{B4.b}$$

We see that in this case equation (24) in Červený and Hron (1980) holds, and therefore their equations (26) and (27) can be used after suitable modifications. We must have

$$\frac{dU_p^{(k)}}{ds} + \frac{1}{2} U_p^{(k)} \left(A\tau_{,jj} + \frac{d \log \rho A^2}{ds} \right) = G_0^{(k)}(s) \tag{B5}$$

with

$$G_0^{(k)}(s) = \frac{A}{2\rho} [L_i \mathbf{U}^{(k-1)} - K_i \mathbf{U}_{\perp}^{(k)}] \tau_{,i}, \tag{B6}$$

where the operators K_i and L_i are defined in (A13).

In order to compute the amplitude coefficients from equation (B5) we need to compute $\nabla^2\tau = \tau_{,ii}$. We shall use the Taylor expansion

$$\tau(s, x_1, x_2) = \tau(s, 0, 0) + \mathbf{q}^T\mathbf{M}\mathbf{q}, \tag{B7}$$

where $\mathbf{q} = (x_1, x_2)^T$, and $\mathbf{M}$ is a complex symmetric 2×2 matrix. We have used the fact that $\tau_{,1} = \tau_{,2} = 0$ along the ray. This follows from the eikonal equation (B1). Along the ray we have

$$\nabla^2\tau = -\frac{1}{A^2}\frac{\mathrm{d}A}{\mathrm{d}s} + \mathrm{tr}\,\mathbf{M}. \tag{B8}$$

With our special interpretation of the coordinate system (s, q), the derivation from (50) to (63) in Červený and Hron (1980) is still valid, and we have

$$\frac{\mathrm{d}\mathbf{M}}{\mathrm{d}s} + A\mathbf{M}^2 = 0. \tag{B9}$$

We want to solve for the zero-order amplitude coefficient $U_p^{(0)} = U_p$ and note that $G_0^{(0)}(s) = 0$ so that (B5) becomes

$$\frac{\mathrm{d}U_p}{\mathrm{d}s} + \frac{1}{2}U_p\left(-\frac{1}{A}\frac{\mathrm{d}A}{\mathrm{d}s} + A\,\mathrm{tr}\,\mathbf{M} + \frac{\mathrm{d}\log\rho A^2}{\mathrm{d}s}\right) = 0. \tag{B10}$$

Changing variable to $V = \sqrt{(\rho A)} \cdot U_p$ gives

$$\frac{\mathrm{d}V}{\mathrm{d}s} = -\frac{A}{2}\,\mathrm{tr}\,\mathbf{M}V \tag{B11}$$

with solution

$$V(s) = V(s_0)\exp\left[-\frac{1}{2}\int_{s_0}^{s}A(\sigma)\,\mathrm{tr}\,\mathbf{M}(\sigma)\,\mathrm{d}\sigma\right]. \tag{B12}$$

Equation (B9) can be simplified if we consider $\mathbf{N} = \mathbf{M}^{-1}$ which gives

$$\frac{\mathrm{d}\mathbf{N}}{\mathrm{d}s} = A \cdot \mathbf{I}, \tag{B13}$$

where $\mathbf{I}$ is a 2×2 identity matrix. Equation (B12) may be replaced by a computationally more convenient expression by using the variable $W = (\det \mathbf{N})^{1/2} \cdot V$. We note that

$$\mathrm{tr}\,\mathbf{M} = \frac{\mathrm{tr}\,\mathbf{N}}{\det \mathbf{N}} \tag{B14}$$

and

$$\frac{\mathrm{d}(\det \mathbf{N})}{\mathrm{d}s} = A\,\mathrm{tr}\,\mathbf{N}. \tag{B15}$$

With these expressions we see that (B11) gives

$$\frac{dW}{ds} = 0,$$
(B16)

so that

$$V(s) = V(s_0) \left[\frac{\det \mathbf{N}(s_0)}{\det \mathbf{N}(s)} \right]^{1/2}.$$
(B17)

Point source

We now assume that the source is a point source at $s = 0$, and that the medium is homogeneous in the vicinity of the source. We let

$$U_0(\omega) = U(1, \omega) \exp\left[-i\omega\tau(1)\right]$$
(B18)

be the displacement at $s_0 = 1$ m (but without the delay due to the 1 m separation from the source point).

The source field is symmetric so that $\mathbf{N}(s_0) = n(s_0) \cdot \mathbf{I}$, and equation (B13) gives

$$[\det \mathbf{N}(s)]^{1/2} = n(s) = n(s_0) + \int_{s_0}^{s} A(\sigma)\, d\sigma.$$
(B19)

We have shown that $\sqrt{(\rho A \det \mathbf{N})}U_p$ is constant. The first-order solution is then

$$U(s, \omega) = \frac{\sqrt{(\rho(s_0)A(s_0) \det \mathbf{N}(s_0))}}{\sqrt{(\rho(s)A(s) \det \mathbf{N}(s))}} U(s_0, \omega) \exp\left[i\omega(\tau(s) - \tau(s_0))\right],$$
(B20)

where $A(s)$, $\mathbf{N}(s)$, and $\tau(s)$ also are functions of ω.

With a point source at $s = 1$ m the displacement for $s \geq 1$ m is given by

$$U(s, \omega) = \sqrt{\left(\frac{\rho(0)A(0)}{\rho(s)A(s)}\right)} \frac{A(0)}{n(s)} U_0(\omega) \exp\left[i\omega\tau(s)\right],$$
(B21)

where $\tau(s)$ and $n(s)$ are given by (see (B2) and (B19))

$$\tau(s) = \int_0^s \frac{d\sigma}{A(\sigma)}$$
(B22.a)

and

$$n(s) = \int_0^s A(\sigma)\, d\sigma,$$
(B22.b)

since $\tau(0) = n(0) = 0$.

Line source

We consider a line source in the x_2-direction. The previous derivation is no longer valid after (B12) where, in this case, $M_{22} = M_{12} = 0$ so that the matrix $\mathbf{N} = \mathbf{M}^{-1}$

does not exist. With $m(\sigma) = M_{11}(\sigma)$, and $M_{22} = M_{12} = 0$, (B9) now gives

$$\frac{dm}{ds} + Am^2 = 0. \tag{B23}$$

We let $n(s) = m(s)^{-1}$, and again $n(s)$ is given by (B19). Equation (B11) now becomes

$$\frac{dV}{ds} = -\frac{A}{2} mV \tag{B24}$$

from which we obtain that $\sqrt{n} \cdot V$ is constant.

The first-order solution is now

$$U(s, \omega) = \sqrt{\left(\frac{\rho(s_0)A(s_0)n(s_0)}{\rho(s)A(s)n(s)}\right)} U(s_0, \omega) \exp [i\omega(\tau(s) - \tau(s_0))]. \tag{B25}$$

When we consider a line source at $s = 0$ with a displacement $U_0(\omega)$ at $s_0 = 1$ m (of the same form as in (B18)), we obtain that the displacement for $s \geq 1$ m is given by

$$U(s, \omega) = \sqrt{\left(\frac{\rho(0)A(0)^2}{\rho(s)A(s)n(s)}\right)} U_0(\omega) \exp [i\omega\tau(s)], \tag{B26}$$

where $n(s)$ and $\tau(s)$ are given in (B22).

Plane source

For a plane source $\mathbf{M}(s_0) = \mathbf{0}$, and (B9) gives $\mathbf{M}(\sigma) = \mathbf{0}$. From (B12) we see that in this case $V(s)$ is constant, and the first-order solution is

$$U(s, \omega) = \sqrt{\left(\frac{\rho(s_0)A(s_0)}{\rho(s)A(s)}\right)} U(s_0, \omega) \exp [i\omega(\tau(s) - \tau(s_0))]. \tag{B27}$$

When we consider a plane source at $s_0 = 0$ with displacement $U_0(\omega)$ we have for $s \geq 0$

$$U(s, \omega) = \sqrt{\left(\frac{\rho(0)A(0)}{\rho(s)A(s)}\right)} U_0(\omega) \exp [i\omega\tau(s)], \tag{B28}$$

where $\tau(s)$ is given by (B22.a).

APPENDIX C

REFLECTION AND TRANSMISSION COEFFICIENTS FOR VERTICALLY TRAVELING WAVES IN VISCOELASTIC MEDIA

We consider two viscoelastic half-spaces in welded contact at $x_3 = z = z_k$. The stress–strain relation (A1) gives

$$\sigma_{33}(x, t) = (\lambda + 2\mu) * u_{3,3}. \tag{C1}$$

When we Fourier-transform this equation and use the definition of the propagation velocity A, we obtain

$$S_{33} = \rho A^2 U_{3,3}. \tag{C2}$$

Spherical waves

We consider a vertically traveling wave of the form (see (B21))

$$U_3(s) = \pm \sqrt{\left(\frac{\rho(0)A(0)}{\rho(s)A(s)}\right)} \frac{A(0)}{n(s)} \exp [i\omega\tau(s)], \tag{C3}$$

where the plus sign is used for a downward traveling wave, and the minus sign is used for an upward traveling wave. This gives

$$S_{33} = \rho A^2 \left[i\omega\tau_{,3} - \frac{1}{n} n_{,3} - \frac{1}{2A\rho} (A\rho)_{,3} \right] U_3. \tag{C4}$$

From (B22) we obtain

$$\tau_{,3} = \pm \frac{1}{A} \tag{C5.a}$$

and

$$n_{,3} = \pm A, \tag{C5.b}$$

where the plus sign refers to a downward traveling wave and the minus sign refers to an upward traveling wave.

We let the displacement be positive in the direction of the ray so that the reflected wave is $-R \cdot U_3$ and the transmitted wave is $T \cdot U_3$ when we refer to the x_3-coordinate system. The boundary conditions require that U_3 and S_{33} shall be continuous at the interface between the two media. This gives

$$T = 1 - R \tag{C6}$$

and

$$\left\{ \rho A^2 \left[\frac{i\omega}{A} - \frac{A}{n} - \frac{(A\rho)_{,3}}{2A\rho} - R \left(\left[-\frac{i\omega}{A} + \frac{A}{n} - \frac{(A\rho)_{,3}}{2A\rho} \right) \right] \right] \right\}_{z=z_{k-}}$$

$$= \left\{ \rho A^2 T \left[\frac{i\omega}{A} - \frac{A}{n} - \frac{(A\rho)_{,3}}{2A\rho} \right] \right\}_{z=z_{k+}}, \tag{C7}$$

where z_{k-} is just above the interface, and z_{k+} is just below the interface.

We assume that the change in $(A\rho)_{,3}$ across the interface is small, so that these terms may be dropped. This gives

$$R = \frac{G(z_{k+}) - G(z_{k-})}{G(z_{k+}) + G(z_{k-})} \tag{C8}$$

with

$$G = \rho A \left(1 - \frac{A^2}{i\omega n} \right). \tag{C9}$$

Cylindrical waves

We now consider a vertically traveling wave of the form (B26)

$$U_3(s) = \pm \sqrt{\left(\frac{\rho(0)A(0)^2}{\rho(s)A(s)n(s)} \right)} U_0(\omega) \exp\left[i\omega\tau(s) \right]. \tag{C10}$$

Equation (C2) then gives

$$S_{33} = \rho A^2 \left[i\omega\tau_{,3} - \frac{1}{2n} n_{,3} - \frac{1}{2A\rho} (A\rho)_{,3} \right] U_3. \tag{C11}$$

The previous derivation may be repeated to give the transmission and reflection coefficients of the same form as in (C6) and (C8), but now with

$$G = \rho A \left(1 - \frac{A^2}{i2\omega n} \right). \tag{C12}$$

Plane waves

A vertically traveling plane wave is of the form (B28)

$$U_3(s) = \pm \sqrt{\left(\frac{\rho(0)A(0)}{\rho(s)A(s)} \right)} U_0(\omega) \exp\left[i\omega\tau(s) \right], \tag{C13}$$

which gives

$$S_{33} = \rho A^2 \left[i\omega\tau_{,3} - \frac{1}{2A\rho} (A\rho)_{,3} \right] U_3. \tag{C14}$$

This gives the plane-wave transmission and reflection coefficients of the same form as in (C8) and (C9) but now with

$$G = \rho A. \tag{C15}$$

Frequency-independent reflection and transmission coefficients

The reflection and transmission coefficients derived above are all functions of frequency, and it is computationally expensive to use them. We shall use the following expression for the complex velocity (see appendix D):

$$A(z, \omega) = C_r(z) \frac{1 + \dfrac{1}{\pi Q} \log \dfrac{\omega}{\omega_r}}{1 + \dfrac{i}{2Q}}, \tag{C16}$$

where Q is constant in each layer. The reflection coefficient is given by (C8), where

$$G(z) = \rho A\left(1 - k\,\frac{A^2}{i\omega n}\right) \tag{C17}$$

with $k = 1$ for spherical waves, $k = 0.5$ for cylindrical waves, and $k = 0$ for plane waves.

A computationally efficient approximation is obtained by using the function

$$G_0(z) = \frac{\rho C_r(z)}{1 + \dfrac{i}{2Q}} \tag{C18}$$

in (C8) and (C6). This gives the frequency-independent plane-wave reflection and transmission coefficients derived in Waters (1978, appendix 4A).

A first-order Taylor expansion of (C8) gives

$$R = \frac{G_0(z_{k+}) - G_0(z_{k-})}{G_0(z_{k+}) + G_0(z_{k-})} + \frac{2G_0(z_{k+})G_0(z_{k-})}{[G_0(z_{k+}) + G_0(z_{k-})]^2}$$

$$\cdot\left\{\left[\frac{1}{Q(z_{k+})} - \frac{1}{Q(z_{k-})}\right]\frac{1}{\pi}\log\frac{\omega}{\omega_r} + \frac{k}{i\omega n}\left[A(z_{k-})^2 - A(z_{k+})^2\right]\right\}. \tag{C19}$$

We see that the approximation is valid if the change in Q across the interface is small, and if the waves are nearly plane (or if the change in complex velocity across the interface is small). The last term in (C17) is a near-field term (Berkhout 1982).

APPENDIX D

COMPLEX PROPAGATION VELOCITY

The complex velocity $A(s, \omega)$ is obtained from the complex bulk-modulus given in (A15.a). We use a bulk-modulus given by Kjartansson (1979), which gives a velocity of the form

$$A(z, \omega) = \frac{C_r(z)\left(1 + \dfrac{1}{\pi Q}\log\left(\dfrac{\omega}{\omega_r}\right)\right)}{\left(1 + \dfrac{i}{2Q}\right)}, \tag{D1}$$

where the quality factor Q is defined by (Aki and Richards 1980, p. 183):

$$\frac{1}{Q} = -\frac{\text{Im}\,(\Lambda + 2M)}{\text{Re}\,(\Lambda + 2M)}, \tag{D2}$$

and $C_r(z)$ is reference velocity measured at frequency ω_r. Q is assumed to be independent of frequency and space coordinates. Equation (D1) is valid when the conditions

$$\frac{1}{Q} \ll 1, \tag{D3.a}$$

and

$$\frac{1}{\pi Q} \log \left(\frac{\omega}{\omega_r} \right) \ll 1 \tag{D3.b}$$

are satisfied. This is the case for most applications. Equation (D1) coincides with the velocity given by Aki and Richards (1980) which was calculated from laboratory measurements of creep-functions. Futtermann (1962) obtained the same relation by using the principle of causality. Laboratory and field measurements (Newman and Worthington 1982, Winkler and Nur 1982) indicate that the amplitudes of seismic waves should depend exponentially on frequency and traveltime. Furthermore, the product of the real part of the velocity $A(z, \omega)$ and the quality factor Q should be approximately independent of frequency. With our solution of the equations of motion and choice of velocity—(1) and (D1), respectively—these requirements are met.

In the numerical calculations we assume that the reference velocity $C_r(z)$ is a linear function of depth:

$$C_r(z) = C + g(z - z_0), \tag{D4}$$

where g is a constant and C_r is assumed to be known at the point z_0.

REFERENCES

AKI, K. and RICHARDS, G. 1980, Quantitative Seismology, W.H. Freeman and Co., San Francisco.

BALCH, A.H., LEE, M.W., MILLER, J.J. and RYDER, R.T. 1982, The use of vertical seismic profiles in seismic investigations of the earth, Geophysics 47, 906–918.

BARANOV, V. and KUNETZ, G. 1960, Film synthétique avec réflexions multiples; théorie et calcul pratique, Geophysical Prospecting 8, 315–325.

BEN-MENAHEM, A. and SINGH, S.J. 1981, Seismic Waves and Sources, Springer-Verlag, New York.

BERKHOUT, A.J. 1982, Seismic Migration, Elsevier, Amsterdam.

BUCHEN, P.W. 1974, Application of the ray-series method to linear viscoelastic wave propagation, Pure and Applied Geophysics 112, 1011–1029.

ČERVENÝ, V. and HRON, F. 1980, The ray series method and dynamic ray tracing system for three-dimensional inhomogeneous media, Bulletin of the Seismological Society of America 70, 47–77.

FUTTERMAN, W.I. 1962, Dispersive body waves, Journal of Geophysical Research 67, 5279–5291.

GANLEY, D.C. 1981, A method for calculating synthetic seismograms which include the effects of absorption and dispersion, Geophysics 46, 1100–1107.

HRON, F. 1972, Numerical methods of ray generation in multilayered media, in Methods in Computational Physics 12, Theoretical Seismology (eds B. Alder, S. Fernbach, and B.A. Bolt), Academic Press, New York.

KAN, T.K., CORRIGAN, D. and HUDDLESTON, P.D. 1981, Attenutation measurements from vertical seismic profiles, preprint of paper presented at the 51st Annual International Meeting of the SEG, Los Angeles, California.

KENNETT, B.L.N. 1979, Theoretical reflection seismograms for elastic media, Geophysical Prospecting 27, 301–321.

KJARTANSSON, E. 1979, Constant Q-wave propagation and attenuation, Journal of Geophysical Research 84, 4737–4748.

NEWMAN, P. 1973, Divergence effects in a layered earth, Geophysics 38, 481–488.

NEWMAN, P.J. and WORTHINGTON, M.H. 1982, In-situ investigation of seismic body-waves in heterogeneous media, Geophysical Prospecting 30, 377–400.

NIELSEN, P.H. 1978, Calculation of synthetic reflection seismograms in the frequency domain, Geophysical Prospecting 26, 399–406.

TROREY, A.W. 1962, Theoretical seismograms with frequency and depth dependent absorption, Geophysics 27, 766–785.

VETTER, J.W. 1981, A forward generated synthetic seismogram for equal-delay layered media models, Geophysical Prospecting 29, 363–373.

WATERS, K.H. 1978, Reflection Seismology, Wiley, New York.

WINKLER, W. and NUR, A. 1982, Seismic attenuation: Effects of pore fluids and frictional sliding, Geophysics 47, 1–15.

WUENSCHEL, P.C. 1960, Seismogram synthesis including multiples and transmission coefficients, Geophysics 25, 106–129.

WYATT, K.D. 1981, Synthetic vertical seismic profile, Geophysics 46, 880–891.